Bull Volcanol (2008) 70:861–875
DOI 10.1007/s00445-007-0175-9

RESEARCH ARTICLE

A model for radial dike emplacement in composite cones based on observations from Summer Coon volcano, Colorado, USA

Michael P. Poland · William P. Moats · Jonathan H. Fink

Received: 3 March 2007 / Accepted: 27 September 2007 / Published online: 6 November 2007

Abstract We mapped the geometry of 13 silicic dikes at Summer Coon, an eroded Oligocene stratovolcano in southern Colorado, to investigate various characteristics of radial dike emplacement in composite volcanoes. Exposed dikes are up to about 7 km in length and have numerous offset segments along their upper peripheries. Surprisingly, most dikes at Summer Coon increase in thickness with distance from the center of the volcano. Magma pressure in a dike is expected to lessen away from the pressurized source region, which would encourage a blade-like dike to decrease in thickness with distance from the center of the volcano. We attribute the observed thickness pattern as evidence of a driving pressure gradient, which is caused by decreasing host rock shear modulus and horizontal stress, both due to decreasing emplacement depths beneath the sloping flanks of the volcano. Based on data from Summer Coon, we propose that radial dikes originate at depth below the summit of a host volcano and follow steeply inclined paths towards the surface. Near the interface between volcanic cone and basement, which may represent a neutral buoyancy surface or stress barrier, magma is transported subhorizontally and radially away from the center of the volcano in blade-like dikes. The dikes thicken with increasing radial distance, and offset segments and fingers form along the upper peripheries of the intrusions. Eruptions may occur anywhere along the length of the dikes, but the erupted volume will generally be greater for dike-fed eruptions far from the center of the host volcano owing to the increase in driving pressure with distance from the source. Observed eruptive volumes, vent locations, and vent-area intrusions from inferred post-glacial dike-fed eruptions at Mount Adams, Washington, USA, support the proposed model. Hazards associated with radial dike emplacement are therefore greater for longer dikes that propagate to the outer flanks of a volcano.

Keywords Radial dike swarm · Intrusion · Composite volcano · Driving pressure · Colorado · Volcanic hazards · Summer Coon

Editorial responsibility: S. Nakada

M. P. Poland (✉)
U.S. Geological Survey, Hawaiian Volcano Observatory,
P. O. Box 51, Hawaii National Park, HI 96718-0051, USA
e-mail: mpoland@usgs.gov

W. P. Moats
Hazardous Waste Bureau,
New Mexico Environment Department District 1,
5500 San antonio, NE,
Albuquerque, NM 87109, USA
e-mail: william.moats@state.nm.us

J. H. Fink
School of Earth and Space Exploration, Arizona State University,
Box 871404, Tempe, AZ 85287-1404, USA
e-mail: jon.fink@asu.edu

Introduction

Magmatic intrusions in volcanic systems are varied in form and often lead to eruptive activity away from the summit of a host volcano. At Hawaiian shields, dikes are typically injected into rift zones that extend from summit calderas (Fiske and Jackson 1972). In contrast, shield volcanoes of the Galapagos archipelago are characterized by dikes that have circumferential and radial orientations with respect to the summit region (Chadwick and Howard 1991). Intrusive

activity at silicic calderas is often concentrated along ring faults as typified by geological mapping at Valles caldera, New Mexico (Smith and Bailey 1968), and historical eruptions at Rabaul, Papua New Guinea (Saunders 2001). Radial dikes with orientations that are subject to regional stress conditions are common at arc stratovolcanoes (Nakamura 1977).

Dike-fed flank eruptions on composite volcanoes have the potential to discharge large volumes of eruptive products, and can be accompanied by highly explosive activity. For example, during the 1669 eruption of Mount Etna, a ~1 km^3 lava flow, probably fed by a radial dike, erupted from a vent 2,500 m below and 15 km distant from the summit, partially burying the city of Catania (Corsaro et al. 1996). Sakurajima volcano, Japan, has experienced several eruptions from radial dikes that simultaneously extended in opposite directions from the summit, including activity in 1476, 1779, and 1914. The 1914 eruption was from both the summit and a WSW-ENE-oriented chain of fissures and craters, and erupted a volume of 2.2 km^3 (1.6 km^3 of which was lava). The lava flowed into the 400 m-wide Seto strait, connecting the island of Sakurajima with the Oosumi peninsula (Omori 1915; Yokoyama 1986; Hashimoto and Tada 1992). A more extreme example, though in a then-unpopulated area, is the 1912 eruption of Novarupta, Alaska, which produced about 30 km^3 of ash fall and ignimbrite deposits in the largest volcanic eruption of the 20th century. The activity was coincident with caldera collapse at Katmai volcano, 10 km distant, suggesting that Novarupta was fed by a dike that propagated laterally away from Katmai (Hildreth and Fierstein 2000; Coombs and Gardner 2001).

These cases exemplify the importance of dike-fed flank activity when considering hazards due to eruptions of composite volcanoes. In particular, hazards assessments would benefit from knowledge of: (1) probable vent location, (2) probable eruptive volume, and (3) potential for detection prior to eruption. Regions with the greatest potential for future flank activity are those where historic and prehistoric dikes and eruptive vents are most common, and can be identified using principles described by Nakamura (1977), who showed that radial dikes will assume paths that are parallel to the most compressive horizontal stress in the crust during emplacement. In contrast, little data exist to constrain other characteristics, such as the probable distance from the summit, volume, and precursory activity of dike-fed flank eruptions.

We investigated radial dike intrusion by studying dike geometry at the eroded Summer Coon volcano in south-central Colorado (Fig. 1), where hundreds of small basaltic-andesite dikes and approximately 20 large silicic dikes are arranged in a radial pattern (Lipman 1968). We measured thicknesses along the lengths of the 13 best-exposed silicic dikes to determine the driving pressures during emplacement, from which we can gain insights into the potential volume and location of a flank eruption. In addition, we inferred the probable geometry of an eruptive fissure at the surface based on the form of the mapped intrusions. The resulting model of radial dike intrusion may be applicable as a tool for forecasting the behavior of dikes and assessing associated hazards at active stratovolcanoes.

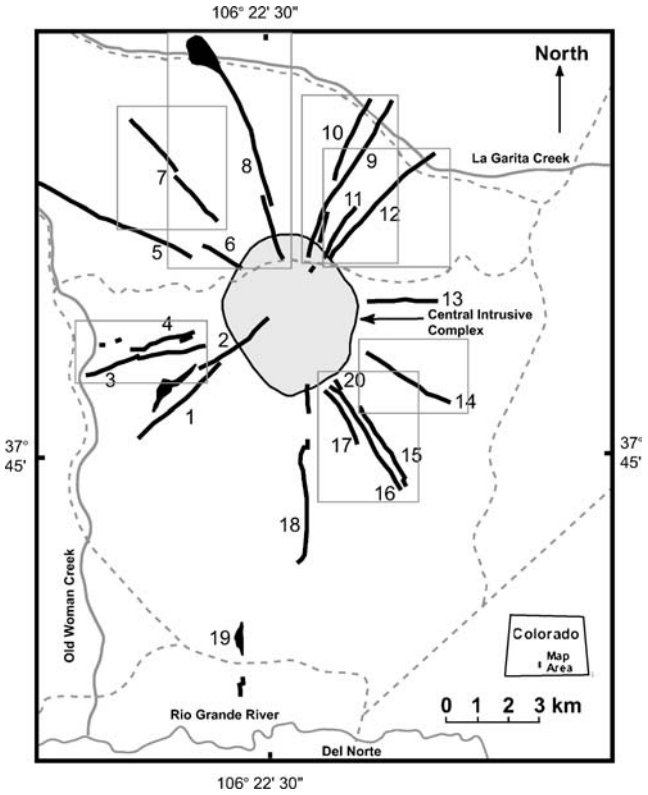

Fig. 1 Sketch map of Summer Coon volcano, located north of the town of Del Norte in southern Colorado, showing access roads (*dashed lines*), rivers and streams (*solid gray lines*), the central intrusive complex of the volcano (*shaded*), and silicic dikes (*numbered 1–20*). The approximate locations of the maps in Fig. 4 are outlined. Modified from Moats (1990)

Geology of Summer Coon volcano

Summer Coon volcano is part of the San Juan volcanic field, which covers 25,000 km^2 in southwestern Colorado and northern New Mexico and contains many silicic calderas and stratovolcanoes. Stratovolcano growth in the San Juan field commenced at about 35 Ma and reached a peak between 30 and 35 Ma, based on K–Ar dating (Lipman et al. 1970). Lipman et al. (1970) dated two dikes at Summer Coon, at 32.4±1.3 and 34.4±1.4 Ma. Perry et al. (1999) reported nine $^{40}Ar/^{39}Ar$ dates that ranged from 32.6 to 33.9 Ma. Seven of the dates are between 33.0 and 33.5 Ma,

Fig. 2 Outward-dipping basaltic-andesite breccias north of the central intrusive complex at Summer Coon volcano. The dip direction to the left indicates that prior to erosion the summit of the volcano was to the right

implying a duration of magmatic activity on the order of several hundred thousand years (Perry et al. 1999).

Erosion has destroyed much of the upper Summer Coon edifice, and only the central intrusive stocks, radial dikes, and some outward dipping extrusive deposits (composed mostly of basaltic-andesite breccias) are preserved (Lipman 1968; Mertzman 1971; Moats 1990; Valentine et al. 2000) (Fig. 2). Lipman's (1976) 1:48,000-scale geological map of the volcano shows the distribution of extrusive and intrusive units, including dikes. Dips of extrusive deposits vary around the volcano, with greater dips on the east flank than on the west. The asymmetric dip distribution and eastward dips of younger, originally horizontal nearby ignimbrite sheets indicate that the volcano was tilted to the southeast at least 5 million years after the cessation of volcanic activity, probably due to the formation of the Rio Grande Rift to the east (Lipman 1968; Mertzman 1971; Moats 1990). Based on a projection of the elevation of outcrops of pre-Summer Coon rhyodacite units along La Garita Creek (Fig. 1), the base of the volcanic cone lies approximately 300 m below the central intrusive complex at the current level of exposure. Oil and gas drilling ~5 km SW of the central intrusive complex suggests that older rocks of the underlying Conejos formation, which are made up of mostly andesitic extrusive and volcaniclastic units, are on the order of 1,200 m thick and underlain by Tertiary and Cretaceous sedimentary rocks (Gries 1985).

Eruptive and intrusive units at Summer Coon range in composition from basaltic-andesite to rhyolite (Lipman 1968; Mertzman 1971; Valentine et al. 2000). Based on cross-cutting relationships between dikes and extrusive deposits, and superposition of flank extrusives, Lipman (1968) divided the compositional evolution of the volcano into three stages: (1) early basaltic-andesite, (2) middle rhyolite, and (3) late-stage dacite, which is consistent with the later interpretation of Mertzman (1971) based on petrologic and geochemical data. Similarly, Valentine et al. (2000) and Perry et al. (2001) favored a sequence including an early mafic phase dominated by basaltic-andesite with minor amounts of rhyolite and dacite, followed by a less voluminous dacite phase.

The most distinguishing characteristic of Summer Coon is the pattern of radial dikes that emanate from the center of the volcano. The dike swarm consists of hundreds of short (~200 m average outcrop length) and thin (~1 m average) basaltic-andesite dikes, and approximately 20 longer (~2–7 km) and thicker (~50 m) silicic (rhyodacite, quartz latite, and rhyolite) dikes (Lipman 1968; Moats 1990; Perry et al. 2001). The mafic dikes are easily eroded and poorly exposed. In contrast, many of the silicic dikes form topographic walls that commonly exceed 20 m in height above the surrounding country (Lipman 1968) (Fig. 3). For ease of reference, Summer Coon dikes in this study are numbered as 1–20 (Fig. 1). Moats (1990) mapped the

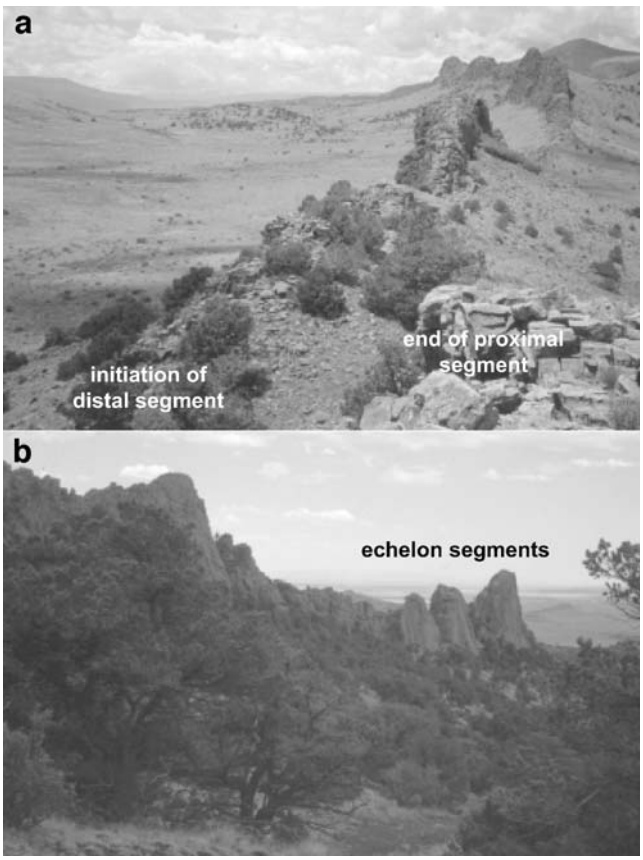

Fig. 3 Examples of segmentation in silicic dikes at Summer Coon. **a** Segment offset of approximately 5 m, looking west along Dike 3. The segments are not connected at the level of exposure. **b** Echelon segmentation along Dike 8, looking south. The dike is continuous at the base of the outcrop, which represents one of two large dike segments, but broken into smaller-scale, secondary segments along the upper surface

geometry of the 13 best-exposed silicic dikes, including thickness, azimuth, and segmentation (Fig. 4). The dikes generally have radial orientations over large distances, suggesting that regional horizontal differential stress was low at the time of dike emplacement (Mertzman 1971; Nakamura 1977). Olson and Pollard (1989) showed that fractures driven only by internal pressurization in an isotropic regional stress field will have an anastamosing geometry characterized by curving crack paths and intersections between adjacent fractures. At Summer Coon, Dikes 9 and 10 (both rhyodacite), as well as Dikes 16 and 20 (both quartz–latite), intersect, and curving dike trends are locally common, implying a relatively isotropic horizontal regional stress field during intrusion.

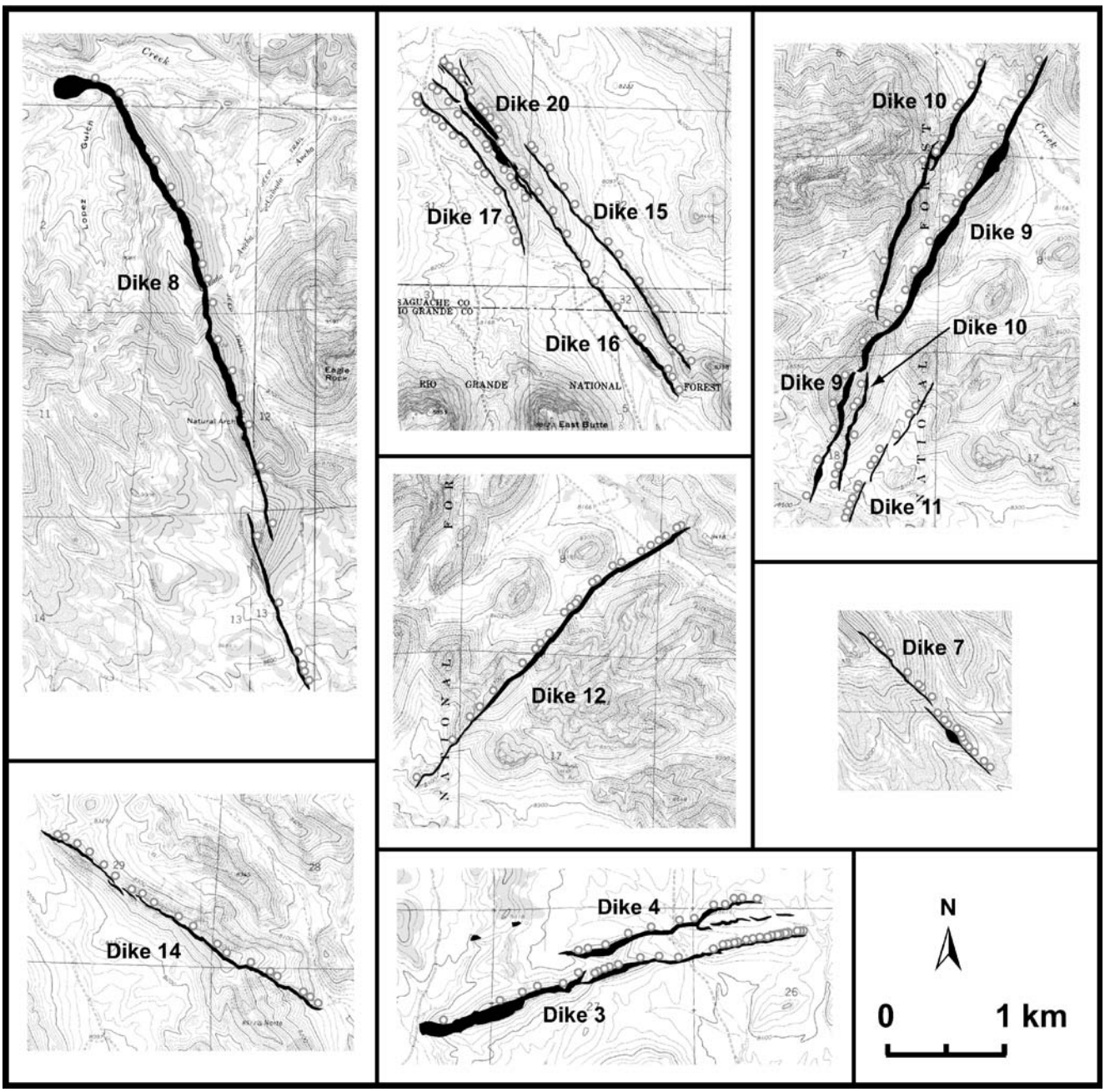

Fig. 4 Maps of 13 silicic dikes at Summer Coon volcano georeferenced to 1:24,000 USGS topographic quadrangles. *A number* designates each dike, and positions within the radial swarm are shown in Fig. 1. Some map areas cover multiple dikes, but only those that fall completely in the map area are shown. *Circles* show locations of thickness measurements. *Zigzag outcrop patterns* visible on several dikes illustrate the multiple scales of segmentation that are common at Summer Coon. Dikes originally mapped by Moats (1990)

Moats (1990) reconstructed the paleotopography of the volcanic cone by projecting up-dip the contact between the basaltic-andesite breccias and silicic lavas around the volcano. The reconstruction gives dimensions for the edifice of approximately 4,200 m in elevation and a basal diameter of 14 km. The cone rose at least 2,200 m above the underlying basement, had a volume of about 110 km^3, and was characterized by an average surface slope of 17°. Projected dimensions are minimum values because they are based on the attitude of a contact near the top of, but still within, the volcanic pile, and do not account for the concave-upward shape that is common near the summits of most stratovolcanoes (Lacey et al. 1981). For comparison, Mount Rainier volcano in Washington rises 2,200 m above the surrounding terrain, and has a basal diameter of 17 km and a volume of 140 km^3 (Sherrod and Smith 1990; Wood and Kienle 1990, p. 158). Moats' (1990) reconstruction can also be used to determine the minimum emplacement depths along the lengths of the dikes, which is necessary to constrain the conditions at the time of dike intrusion. Much of the work described below makes use of field measurements by Moats (1990).

Dike thickness

A key factor in the consideration of hazards due to volcanic eruption is potential eruptive volume. For central vent eruptions, the volume of erupted products will depend on a range of variables, including magma composition, volatile content, temperature, and conduit and vent dimensions. For dikes, intrusion driving pressure (defined as the difference between the magma pressure and the horizontal stress perpendicular to the plane of the dike) is a key element. Assuming intrusions that are relatively similar (with respect to temperature, composition, viscosity, etc.), a dike with a higher driving pressure can deliver more magma to the site of a surface eruption than a dike with a lower driving pressure. Thickness is directly related to driving pressure (Pollard and Muller 1976; Delaney and Pollard 1981; Pollard 1987), so dike thickness can provide important constraints on the potential volume of a dike-fed eruption (Gudmundsson and Brenner 2005). Of course, estimating the thickness of a subsurface dike is problematic, especially during a volcanic crisis; therefore, we attempt to constrain those factors that control dike thickness that can be observed or inferred.

At Summer Coon, most of the well-exposed silicic dikes are teardrop-shaped in plan view, with thicknesses that increase with distance from the central intrusive complex (Moats 1990). Dike thicknesses proximal to the central intrusive complex average ~10 m, but reach up to 40 m near their distal ends before tapering (Fig. 4). Dikes that increase in thickness have also been observed in Hawaii and the British Tertiary Province, though the thickness increase is usually much smaller and occurs over longer distances than observed at Summer Coon (Rubin 1990). Plugs that can be over 100 m thick characterize some Summer Coon dikes at their terminations (e.g., Dikes 2, 8, and 19; Figs. 1 and 4), and at least one intrusion (Dike 7; Fig. 4) hosts a smaller plug closer to the center of the volcano. These plugs may represent locations where magma fed surface eruptions, since dike-fed eruptions generally become focused at one or a few points soon after they begin (e.g., Richter et al. 1970). The observation of increasing thickness with distance from the source is surprising, and indicates an increase in driving pressure with distance. In the absence of significant topography, stress heterogeneities, and variations in host rock properties, dike driving pressure should decrease with distance from the source reservoir (Pollard and Muller 1976; Delaney and Pollard 1981). Identifying the cause of driving pressure increase with distance from the center of the volcano at Summer Coon is critical to understanding the behavior of radial dikes there and at other composite volcanoes, and associated hazards from potential dike-fed flank eruptions at currently active volcanic centers.

Models of dike driving pressures at Summer Coon

Pollard and Muller (1976) and Delaney and Pollard (1981) presented analytical solutions relating dike thickness to driving pressure. Assuming the host rock behaves as a homogenous, elastic solid, the thickness (t) of a blade-shaped dike with a constant driving pressure is described by:

$$t = 2(P - S)\left(a^2 - x^2\right)^{1/2}\left(\frac{1-\upsilon}{\mu}\right) \quad (1)$$

where P is the magma pressure, S is the dike-normal stress (generally the least compressive stress in the crust), a is the half-length of the dike, x is the distance from the along-strike midpoint of the dike, μ is the elastic shear modulus, υ is Poisson's ratio, and driving pressure is defined by $P-S$ (Pollard and Muller 1976; Delaney and Pollard 1981; Pollard 1987; Reches and Fink 1988). Equation 1 predicts an elliptically shaped dike in plan view, unlike the observed teardrop-shaped intrusions at Summer Coon. Weertman (1971) suggested that asymmetry of a fluid-filled crack is caused by a gradient in stress or pressure (which we refer to as a driving pressure gradient) along the fracture. Pollard and Muller (1976) and Delaney and Pollard (1981) described the thickness distribution of a teardrop-shaped dike to be a function of both uniform driving pressure plus

a driving pressure gradient, modifying Eq. 1 to include an additional expression:

$$t = \underbrace{2(P-S)(a^2-x^2)^{1/2}\left(\frac{1-\upsilon}{\mu}\right)}_{\text{constant pres. term (Eq. 1)}} + \underbrace{\nabla(P-S)x(a^2-x^2)^{1/2}\left(\frac{1-\upsilon}{\mu}\right)}_{\text{pres. gradient term}} \quad (2)$$

where ∇ $(P–S)$ is the driving pressure gradient along the dike (see also Pollard 1987).

We model the driving pressure during dike emplacement using a least squares linear inversion to determine both the uniform driving pressure (Eq. 1) and the combination of uniform driving pressure and driving pressure gradient (Eq. 2) that best fit the observed thickness distributions of 13 well-exposed silicic dikes at Summer Coon using measurements collected by Moats (1990) (thickness measurements were not taken at the other seven silicic dikes due to poor exposures). The models assume that a dike can be approximated by a static fluid-filled crack in equilibrium with an elastic media. Although clearly an oversimplification, the analysis can provide useful insights into the emplacement of radial dikes at Summer Coon provided non-equilibrium and inelastic processes do not control the dynamics of dike emplacement. Such processes include: (1) inelastic deformation of the host rock, (2) significant wall-rock erosion by flowing magma or thermal erosion, (3) intrusion along preexisting fractures, (4) irregular geometry in the third dimension (vertical, at Summer Coon), and (5) dike growth in multiple phases or transient pressure changes due to eruptions, (Pollard and Muller 1976; Valentine and Krogh 2006).

Our observations of Summer Coon dikes suggest that while non-equilibrium and non-elastic processes are clearly present, they probably are not major factors in the emplacement of the km-scale intrusions. There is no evidence for welding or significant pore-space closing in host rock adjacent to dike walls that indicates widespread permanent inelastic deformation (Valentine and Krogh 2006). Host rock xenoliths are present in some dike margins but are not especially common, suggesting that wall-rock erosion is not a significant process. We see no evidence that the dikes were intruded along existing fractures and no regional joint or fault sets are known that would influence dike emplacement within or at the base of the Summer Coon edifice. The third dimension of dike geometry cannot be known from the current exposure; however, thermal and mechanical considerations argue for a blade-like shape (Rubin and Pollard 1987; Rubin 1990; 1993; 1995), which would minimize geometrical irregularities in the third dimension. Finally, we believe that multiple intrusion pulses and transient pressure changes due to eruption are not common processes at Summer Coon. Cooling margins, which can indicate multiple intrusive events over time (Gudmundsson 1984), are not present within dike interiors, and the variable flow directions that Poland et al. (2004) measured in the interior of Dike 8 can be explained by localized effects of magma flow in an established dike. At least two of the dikes we analyzed (Dikes 7 and 8) host plugs that may have fed eruptions, and one dike we did not examine in detail (Dike 2) is clearly connected to a rhyolite lava flow. For the bulk of Summer Coon dikes we examined, however, evidence for or against surface eruption is ambiguous. Geologic mapping suggests that the majority of dikes in mafic volcanic systems do not reach the surface to feed eruptions (Gudmundsson 1984; Gudmundsson et al. 1999). Historical activity also suggests that most dikes do not erupt, for instance, the 1975–1984 Krafla rifting episode, which included at least 20 episodes of dike intrusion (inferred form geodetic data) and nine eruptions (Sturkell et al. 2006). The ratio of eruptive to non-eruptive dikes in more silicic systems, like Summer Coon, is unknown, although volcanic unrest (which often involves dike intrusion) is certainly more common than eruption (Newhall and Dzurisin 1988) implying that many of the exposed dikes at Summer Coon did not erupt.

Determining the precise value of μ for in situ Summer Coon rocks is difficult; therefore, we attempted to place realistic bounds on the parameter. Laboratory estimates of μ are as high as 70 GPa, but the rocks of a pervasively fractured and altered volcanic edifice will have different properties than laboratory samples. Schultz (1993) used an elastic shear modulus of 4–23 GPa for a volcanic edifice and Rubin and Pollard (1987) estimated 1–6 GPa for the upper few kilometers of Kilauea volcano in Hawaii. In poorly consolidated sediments, μ can be less than 1 GPa (Nunn 1996). We feel that a range of 1–4 GPa is appropriate for the basaltic-andesite breccias that make up much of the Summer Coon edifice. For Poisson's ratio, we follow both Pollard (1987) and Schultz (1993), who found that 0.25 is reasonable for a rock mass at the scale of a kilometer-long dike. Despite uncertainty in the values of the elastic parameters, particularly the shear modulus, the modeled driving pressures for Summer Coon dikes are comparable to one another because the dikes were emplaced in similar country rock (Moats 1990).

Most dikes at Summer Coon are characterized by 2–4 major segments that can be subdivided into 10–20 minor segments (Moats 1990) (Figs. 3 and 4). Delaney and Pollard (1981) analyzed a dike with 35 segments at Ship Rock, New Mexico, using models based on Eqs. 1 and 2 treating the intrusion as 35 individual cracks, 10 individual cracks, and a single crack. They found that the single crack model had the lowest standard error of the three and probably

gives a lower bound on the magnitude of the driving pressure. Similarly at Summer Coon, models treating a dike as more than one crack produce no significantly better fit than single crack models; therefore, we treat each dike as a single crack, regardless of the number of segments. Because thickness measurements were not collected at segment tips (Fig. 4), local thinning at segment terminations should not influence the results of the inversion. The lack of dependence on the number of segments is an important result, as it suggests that segmentation only affects a minor proportion of the volume of the intrusion, and that the dikes are not segmented at greater depths.

For relatively long, well-exposed dikes at Summer Coon, we find that the driving pressure gradient model (Eq. 2) provides the best explanation of the measured distribution of dike thicknesses (Table 1 gives model results, and Fig. 5 is an example of model fits to thickness measurements from Dike 12). A statistical *F*-test compares the fits of the constant pressure and driving pressure gradient models by accounting for the decreased degrees of freedom in the driving pressure gradient model due to the addition of a second model parameter. If the driving pressure gradient model fits the data significantly better than the constant pressure model at the 95% confidence level, the *F* value will be higher than the 95% threshold (noted in Table 1 as $F_{0.05}$). For Dikes 3, 4, and 7–12, the driving pressure gradient model is a significantly better fit to the data than the constant pressure model. For Dikes 14–17 and 20, however, the driving pressure gradient model does not explain the data significantly better than the constant driving pressure model. Potential error sources in the inversion include (1) incomplete exposure of the dike (dike ends may be concealed, which would yield a minimal dike length) and (2) errors in thickness measurements, which we do not consider since measurement error was not quantified by Moats (1990).

Moats (1990) noted that Dikes 17 and 20 are relatively short and do not reach the outer flanks of the volcano (Fig. 4). Short dikes are likely to have less overall variation in driving pressure; therefore, the constant pressure model should better explain the dike thickness (Table 1). Dike 15 is also poorly explained by the driving pressure gradient model compared to the constant driving pressure model; however, its proximal and distal ends are buried by alluvium (Moats 1990). If the concealed dike terminations taper in thickness, both models would have improved fits. A similar effect may influence the driving pressure gradient's poor approximation for Dike 16, which is parallel to and within 100 m of Dike 15. Finally, the lack of a significantly better fit to Dike 14 thicknesses by the driving pressure gradient model is due to the anomalous thickness of the dike at its proximal end. If the segment of Dike 14 closest to the central intrusive complex is omitted from the analysis, the driving pressure gradient model provides a better approximation of the remaining thickness distribution. The thick proximal segment may represent a pulse of magma after initial dike emplacement, a small plug that transported magma towards the surface, or some other process that is not appropriate for analysis by elastic models.

Modeled driving pressures range from about 8–37 (using μ=1 GPa) to 19–148 (μ=4 GPa) MPa. For dikes that are better explained by the gradient model, the driving pressure gradient varies between 0.003–0.033 (μ=1 GPa) to 0.011–0.133 (μ=4 GPa) MPa/m. For comparison, Pollard and Muller (1976) modeled driving pressures of 3.5–48 MPa for

Table 1 Results for inversions of dike thickness using (1) a constant driving pressure model (Eq. 1 in text) and (2) a constant driving pressure plus a gradient model (Eq. 2 in text)

Dike Number	Number of meas.	Constant pressure			Constant pressure plus a gradient				*F* test		RSS/($n-p$)	
		Pres. (MPa)	RSS	Corr.	Pres. (MPa)	Grad. (MPa/m)	RSS	Corr.	*F* value	$F_{0.05}$	Const	Grad
3	31	8.4–33.8	2,155.2	0.70	10.4–41.8	0.009–0.036	1,032.1	0.86	31.56	4.18	79.8	39.7
4	12	24.2–96.9	1,711.8	0.58	25.6–102.6	0.033–0.133	996.2	0.78	7.18	4.96	155.6	99.6
7	18	7.7–30.9	188.0	0.37	7.9–31.7	0.01–0.06	130.9	0.63	6.98	4.49	20.6	20.6
8	21	9.7–38.8	7,166.6	0.25	9.7–38.8	0.005–0.024	4,199.9	0.69	13.42	4.38	355.8	221.0
9	21	16.8–67.1	7,618.3	0.57	17.4–69.5	0.009–0.038	4584.9	0.74	12.57	4.38	380.9	241.3
10	18	9.3–37.2	1,782.8	0.37	9.1–36.4	0.004–0.017	1,030.2	0.54	11.69	4.49	104.9	64.4
11	12	7.9–19.5	40.5	0.32	4.6–18.5	0.007–0.027	25.2	0.47	6.07	4.96	3.7	2.5
12	23	11.8–47.1	2,564.4	0.56	13.4–53.7	0.014–0.057	496.9	0.94	87.38	4.32	116.6	23.7
14	22	8.4–33.5	1,137.9	–0.22	8.5–34.0	0.003–0.013	1,035.3	0.01	1.98	4.35	54.2	51.8
15	13	9.1–36.5	347.2	0.11	9.1–36.3	0.003–0.011	335.4	0.16	0.39	4.84	28.9	30.5
16	19	8.8–35.3	2,437.3	–0.43	8.7–34.9	0.004–0.015	2,282.4	−0.20	1.15	4.45	135.4	134.3
17	13	11.7–46.9	159.8	0.43	11.8–47.3	0.014	150.5	0.51	0.68	4.84	13.3	13.7
20	15	37.1–148.5	3,422.4	0.70	37.1–148.3	0.012–0.018	3,314.8	0.71	0.42	4.67	244.5	255.0

Grad.=Gradient; Pres.=Pressure; Meas.=Measurements; Corr.=correlation coefficient; RSS=residual sum of squares; n=number of measurements; p=model parameters; (n–p)=degrees of freedom

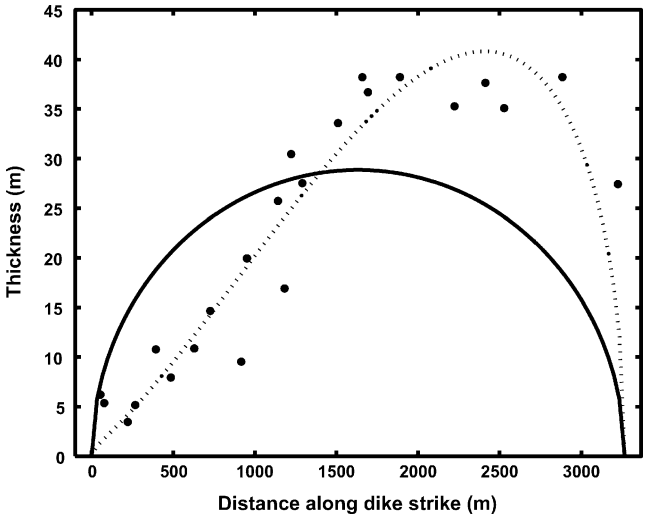

Fig. 5 Plot of along-strike thickness of Dike 12 versus distance (*black dots*) with best-fitting constant pressure (*solid curve*) and constant pressure with a gradient (*dotted curve*) models. The constant pressure plus gradient model is the best fit to the data, indicating that a gradient in driving pressure existed along the length of the dike during intrusion

the Walsen Dike, an intermediate-composition intrusion of the Spanish Peaks radial swarm in Colorado, and 36–500 MPa for the Theater Canyon Sill, composed of diorite porphyry and located in Montana, with driving pressure gradients of 5.2×10^{-5} to 7.1×10^{-4} MPa/m and 0.084 to 1.2 MPa/m, respectively. They noted that the model results for the Walsen dike are reasonable, but the Theater Canyon Sill results are too high, probably because the intrusion was in transition to a laccolith, causing displacements that cannot be approximated by elastic modeling. Dike driving pressures found by other workers generally fall in the range of a few MPa to slightly over 10 MPa (e.g., Delaney and Pollard 1981; Rubin and Pollard 1987; Rubin and Pollard 1988; Delaney and Gartner 1997; Buck et al 2006), which is required to overcome the in-situ fracture toughness of the host rock, estimated at ~100 MPa·m$^{1/2}$ (e.g., Delaney and Pollard 1981), and open the walls of the dike. The lower bounds of modeled driving pressures for most Summer Coon dikes are consistent with these previous estimates, suggesting that elastic models of dike opening are appropriate at Summer Coon, and that μ was relatively low (probably close to 1 GPa).

Sources of driving pressure gradients at Summer Coon

Driving pressure gradients in a dike have several possible sources, including: (1) a regional stress gradient along the dike, (2) systematic variation in magma pressure along the dike, (3) decreasing horizontal stress due to lessening overburden thickness under a sloping ground surface, and (4) host rock heterogeneity along the length of the dike (Pollard and Muller 1976). The first two possibilities cannot explain the modeled driving pressure gradients at Summer Coon. The near-perfect radial pattern of the dike swarm suggests that regional horizontal stress was nearly isotropic at the time of dike emplacement. Variation in magma pressure is generally caused by overpressure in the source reservoir that is transmitted along a dike. The pressure would tend to decrease with distance (Pollard and Muller 1976), causing a dike to thin towards its distal termination (the opposite of what is observed at Summer Coon).

The modeled pressure gradients in Summer Coon dikes can be explained by considering the proximity of the dikes to the ground surface and changes in host-rock properties along the lengths of the dikes. Emplacement depth estimates by Moats (1990) show that many Summer Coon dikes extend laterally to locations that were probably less than 100 m below the ground surface of the volcanic edifice. Most models of dike propagation, including our analysis, ignore the effects of the ground surface and approximate the problem as a pressurized crack in an infinite elastic medium. Pollard and Holzhausen (1979) examined the effect of a free surface on a propagating fracture and found that the resistance to crack dilation decreases as an intrusion approaches the surface and the overburden thickness lessens. These results were confirmed by Rivalta and Dahm (2006) who, through theoretical and laboratory work, showed that resistance to opening decreases as a fluid-filled fracture approaches a free surface. A shallow dike will therefore be thicker in cross section than a deep dike with the same driving pressure, and a dike propagating laterally under a sloping ground surface will become thicker with distance from the center of the volcano as it approaches the surface. Moats (1990) estimated a surface slope (α) of 17° for Summer Coon. Under conditions of hydrostatic stress, the horizontal stress is proportional to the overburden thickness; therefore, the horizontal stress gradient (ΔS_y) is related to the surface slope by:

$$\Delta S_y = \rho\, g\, \tan\alpha \qquad (3)$$

where ρ is the density of the host rock and g is the acceleration due to gravity (Obert and Duvall 1967, p. 495). The density of the basaltic-andesite breccia that makes up most of the volcano may be as high as 2,800 kg/m^3 (Moats 1990), although we suggest a lower bound of 2,000 kg/m^3 to account for the fractured nature of the edifice rocks (Valentine et al. 2000). Using a gravitational acceleration of 9.8 m/s^2, the maximum horizontal stress gradient due to surface slope is 0.006–0.008 MPa/m, which is similar in magnitude to the lower bounds of the gradients we model at Summer Coon (Table 1).

Although the host rock is relatively homogenous at the km-scale of Summer Coon dikes, elastic properties are likely to vary with depth. Compaction due to the weight of overlying rock will seal fractures and decrease pore space within the edifice. However, rock near the surface may host open fractures because the overburden is relatively thin (Rubin and Pollard 1987), resulting in a lower elastic shear modulus. Laboratory experiments of air-filled fracture propagation in layered media indicate that dilation increases as a fracture propagates from a stiff to a more compliant region (Rivalta et al. 2005), and field observations of changes in dike thickness as dikes intrude different lithologies are common (e.g., Baer 1991). The reason for the relationship between thickness and elastic shear modulus is apparent from Eqs. 1 and 2, which show that shear modulus (μ) is inversely proportional to dike thickness. Thus, a minor decrease in μ, for example, by a factor of 2 (which is well within the range of possible variations estimated for other volcanoes, as described above), would cause a corresponding factor of 2 increase in dike thickness. We suggest that a combination of decreasing horizontal (dike-perpendicular) stress as the overburden thickness lessens with shallowing depth and decreasing shear modulus for near-surface rocks is the most likely explanation of the outward thickening of the long silicic radial dikes at Summer Coon. Although only two-dimensional, our relatively simple modeling provides important insights into dike emplacement, and provides a framework and motivation for more complex three-dimensional numerical models of dike propagation within a volcanic edifice.

Dike segmentation

The observed or inferred geometry of an igneous intrusion is commonly used to deduce propagation direction, which is important for assessing the probable location of a radial dike eruption on a stratovolcano, the expected pattern of deformation above the intrusion, and the probable vent configuration if an eruption occurs. Segmented, en echelon geometries are common on both dikes exposed by erosion (e.g. Delaney and Pollard 1981; Klügel et al. 2005), and inferred from surface eruptive vents and fissures (e.g. Pollard et al. 1983; Fink and Pollard 1983; Reches and Fink 1988). Echelon fractures have been noted at a variety of scales in many materials (Pollard et al. 1982), although the mechanism for segment formation is ambiguous. The geometry of offset segments has been used as an indicator of dike propagation direction (e.g., Pollard et al. 1975; Delaney and Pollard 1981); however, Poland et al. (2004) demonstrated that flow directions preserved in chilled dike margins at Summer Coon often do not agree with propagation paths inferred from segmentation.

Moats (1990) recognized three scales of dike segmentation at Summer Coon. The first is characterized by stepping segments on the order of 2 km long that are en echelon, may overlap (for example, Fig. 3a) and are sometimes connected by strands of igneous material (for example, Dikes 3, 7, 8, and 10 in Fig. 4). Second- and third-order segments range in length from ~20 to ~500 m, are often coalesced, and have the appearance of igneous fingers, similar to those described by Pollard et al. (1975) at the periphery of igneous intrusions (for example, stepping segments above the continuous intrusion on Dike 8 in Fig. 3b and the zigzag pattern that is apparent in the map view of Dike 14 in Fig. 4). The amount of segment rotation relative to the trend of the dike does not correlate with either distance from the central intrusive complex or emplacement depth (Moats 1990).

Numerous mechanisms have been invoked to explain the formation of offset dike segments, including principal stress rotation about a vertical axis with decreasing depth (e.g., Sommer 1969; Pollard et al. 1975; Delaney and Pollard 1981), heterogeneous regional stress (e.g., Ode 1957; Muller and Pollard 1977; Pollard et al. 1982; Pollard et al. 1983), intrusion into preexisting fractures (e.g., Gudmundsson 1984; Delaney et al. 1986; Baer and Beyth 1990; Delaney and Gartner 1997), variation in host rock material properties (e.g., Gudmundsson 1983; 1987; Walker 1987; Baer 1991), variation in host rock rheological properties (Reches and Fink 1988), magmatic infiltration of co-intrusion, dike-parallel joints (Olson and Pollard 1991), and changes in the geometry of the magmatic plumbing system with depth (Smith 1987).

Evidence from Summer Coon regarding the mechanism of dike segment formation is ambiguous. Regional horizontal stress at the time of dike emplacement appears to be nearly isotropic, host-rock composition does not vary significantly, and there are no known preexisting fracture sets that explain the varied segment orientations. Another possibility for the ubiquitous segmented dike geometry is intrusion into coeval fractures. Dike propagation is accompanied by the formation of subparallel extensional fractures above and ahead of the intrusion (Delaney et al. 1986; Rubin and Pollard 1988). If magma infiltrates these fractures, offsets will form along the upper surface of the dike. Where the driving pressure is high, the offset segments may propagate towards one-another and their tips may interact as adjacent segments begin to overlap (Olson and Pollard 1991). This model requires some component of subhorizontal crack propagation (in the case of segments that are offset in plan view) and interaction of crack tips. Lateral dike propagation at Summer Coon is supported by magma flow measurements (Poland et al. 2004), and major segment tips curve towards one another at several locations (Fig. 4). Further, from Eq. 6 of Delaney et al. (1986) and

the low end of the modeled driving pressures of Summer Coon dikes (Table 1), the maximum distance normal to a dike at which coeval, parallel fractures should form is on the order of 100–200 m. The largest echelon offset at Summer Coon is a right step of 150 m in the southern portion of Dike 8 (Fig. 4). Based on these factors, interaction with coeval fractures could explain the observed dike segmentation pattern, though other factors, like those described above, may also control or contribute to the process. Regardless of the specific formation mechanism(s) for offset dike segments, it is clear from this and other studies that segmentation is common in tabular intrusions, occurs along the periphery of an intrusion, and may be manifested at the surface by fracture patterns prior to dike-fed eruptions.

Inferred dike emplacement process

Two alternative models for radial dike emplacement can explain the outcrop pattern of silicic dikes at Summer Coon: (1) dikes are planar or fan-shaped (in vertical cross section) and propagated upwards along steep paths from a source at depth (Fig. 6a), and (2) the dikes are blade-shaped and originated from a source below the base of the volcano, ascending along steep trajectories until reaching the base of the edifice (or a neutral buoyancy surface or stress barrier) when dike propagation assumed a subhorizontal path (Fig. 6b).

The first model for radial dike emplacement requires that magma flow be steeply inclined or subvertical along the lengths of the dikes, which will have fan or planar cross-sectional shapes (Fig. 6a). Two lines of evidence contradict this model. First, magma flow, while complex, appears to have been dominantly lateral at Summer Coon (Poland et al. 2004). Second, Rubin (1993; 1995) noted that dikes, especially those that are rhyolitic in composition and have large height to length ratios, are likely to freeze before propagating far from their sources unless the thermal gradient is very low. Summer Coon silicic dikes, which can be up to 7 km in length, were emplaced at shallow levels near a magma reservoir where the thermal gradient is likely to be quite high; thus, planar or fan-like shapes are not the favored intrusion geometry. In contrast, a blade-like form will preserve the high source pressure and is the most thermally efficient shape for transporting silicic magma (Rubin 1993; 1995).

Preferred model for radial dike intrusion

The second model for radial dike emplacement is most consistent with our observations and the magma flow measurements of Poland et al. (2004), which suggest steeply inclined flow proximal, and subhorizontal flow distal, to the central intrusive complex (except where locally influenced by dike segment formation and propagation). At Summer Coon, dikes cannot be mapped into the central intrusive complex at the current level of exposure, probably because they intersect their sources at depth, as indicated by magnetic surveys (Mertzman 1971). This evidence suggests that the dikes originated at depth beneath the volcanic cone, propagating steeply upwards, perhaps along or within the central conduit of the volcano, before assuming lateral paths somewhere near the base of the edifice (Fig. 6b). A similar model has been proposed for the Sunlight volcanic center, an eroded stratovolcano in northwest Wyoming. Based on outcrop configurations and cross cutting relationships, Parsons (1939) speculated that magma flow in radial dikes at Sunlight volcano was steeply inclined within ~800 m of the center of the volcano, but became subhorizontal towards the flanks of the edifice with increasing radial distance.

The shift from upward to outward dike propagation may be caused by either a neutral buoyancy zone or a stress barrier, both of which could occur near the boundary between the volcanic edifice and rocks below. Ryan (1987)

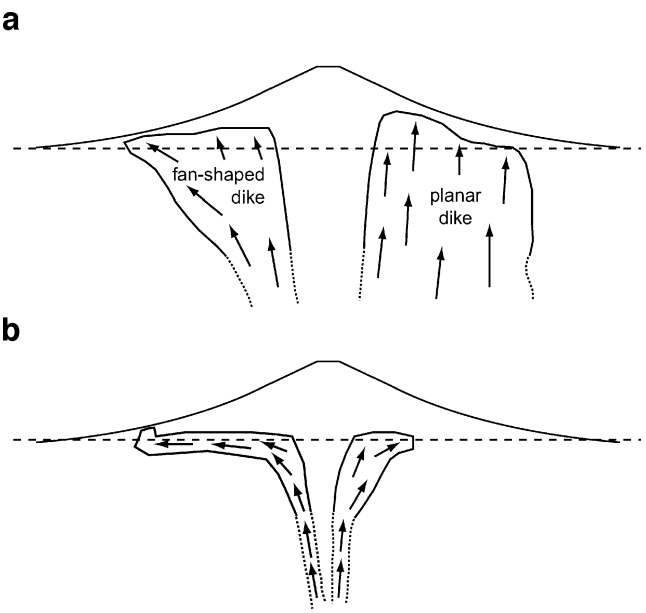

Fig. 6 Schematic cross sections showing possible development of radial dikes at Summer Coon volcano. The dashed horizontal line denotes the current erosional surface at Summer Coon. **a** Radial dikes are planar or fan-shaped and originate from depth below the volcano. Planar or fan-shaped intrusions are not the preferred form for silicic radial dikes because the large contact area between the dike and country rock would probably cause the intrusion to solidify before it propagated far. **b** The favored model for radial dike emplacement. Dikes propagate steeply upwards from depth, becoming subhorizontal upon reaching the base of the volcanic edifice. Extensions of dikes at depth are uncertain and shown by *dotted lines*

cited neutral buoyancy as a probable cause for magma accumulation beneath both mafic and silicic volcanic centers. The density contrast between the rocks of the Summer Coon cone and underlying andesitic Conejos formation (about 300 m below the present exposure) is probably small, suggesting that neutral buoyancy does not play a major role in dike propagation at Summer Coon. Differences in the mechanical behavior of edifice versus basement rock can, however, create a stress barrier along which vertical magma transport transitions to lateral (Gudmundsson and Brenner 2004; 2005).

A stress barrier may also be created by the load of the volcano, as suggested by the numerical modeling of Pinel and Jaupart (2000, 2004) and Martel (2000). The presence of a surface load creates tension at depth and enhances dike propagation, but also increases the vertical compressive stress at the base of the volcano, which can trap dikes before they reach the surface. In a volcano with a size comparable to Summer Coon, only an intrusion with a magma density that is suitably low (due to high silica content, high volatile content, or both) can reach the surface (Pinel and Jaupart 2000). Otherwise, ascending dikes may propagate laterally at shallow depths in a blade-like form, as observed in volcanic constructs in Hawaii and Iceland (Rubin and Pollard 1987; Rubin 1990; Martel 2000). Given the large size of the volcano, the formation of a stress barrier at depth may have caused the change from subvertical to subhorizontal dike propagation at Summer Coon.

Vertical dike propagation that transitions to lateral has been documented at several active volcanoes. At Vesuvio, Italy, 36 radial fissures on the flanks of the volcano formed between 1694 and 1944, and at least 26 are known to have propagated laterally away from the central conduit of the volcano. These radial dikes must have risen vertically beneath the summit before propagating laterally away from the center of the volcano, as suggested by the presence of magma in the bottom of the crater during flank eruptions (Acocella et al. 2006). Between February 2000 and September 2003, Piton de la Fournaise volcano on Reunion Island (Indian Ocean) erupted 11 times, including 9 flank eruptions. For the flank eruptions, seismic and geodetic data suggest rapid vertical magma transport followed by slower lateral dike propagation (Fukushima et al. 2005; Peltier et al. 2005). In May 1991, continuous tilt observations at Unzen volcano, Japan, suggested that vertical magma ascent was interrupted by the formation of a radial dike. The dike stalled after 2 days and vertical ascent resumed, leading to the formation of a dacite lava dome at the volcano's summit (Yamashina and Shimizu 1999). Also in Japan, geodetic and seismic data from the 1998 seismic swarm off the Izu Peninsula has been modeled as vertical magma transport followed by horizontal dike propagation (Morita et al. 2006).

As the dikes propagated laterally away from the center of Summer Coon, the emplacement depth and elastic strength of the rock decreased, causing an increase in the driving pressure and corresponding increase in dike thickness. A thicker dike with higher driving pressure can supply more magma to the site of a surface eruption (Gudmundsson and Brenner 2005), so relatively high

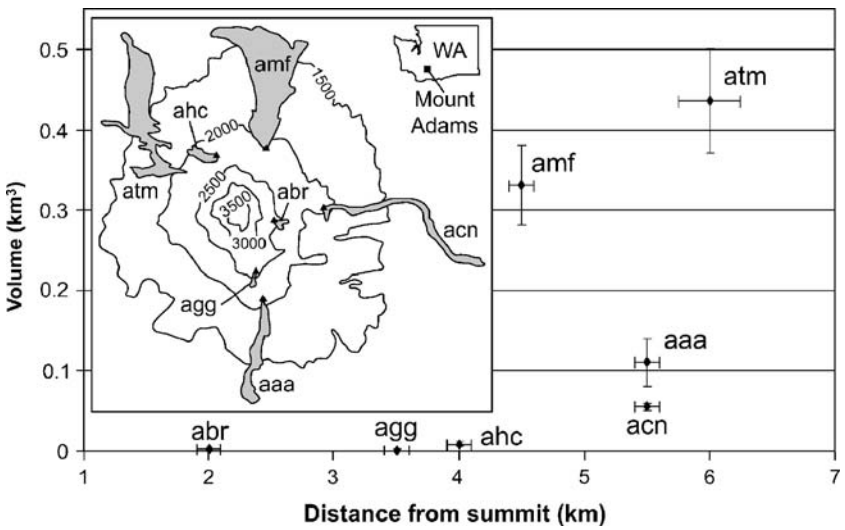

Fig. 7 Plot of erupted volume versus radial distance from the summit for seven post-glacial andesite flows at Mount Adams, Washington. *Inset* shows locations of vents (*triangles*) and lava flows (*shaded*) on Mount Adams. Vent for flow atm is obscured. Unit labels and map are from Hildreth and Fierstein (1995; 1997). The eruptions are assumed to have been fed by radial dikes. Within 4 km of the summit, small-volume eruptions tended to occur while larger volumes erupted at greater distances. The data support the proposal that the potential eruptive volume from a radial dike increases with distance from the center of the host volcano. Data are from Hildreth and Fierstein (1995; 1997). *Contours* show elevation in meters above sea level

volume eruptions are possible far from the summit of the edifice. A few long dikes at Summer Coon terminate in large (~100 m thick) plugs that possibly fed surface eruptions. A plug emanating from Dike 7 is not located on the intrusion termination (Fig. 4) and may have fed an eruption high on the flank of Summer Coon, but its small size suggests that it transported a relatively smaller volume of magma to the surface. Our observations imply that longer radial dikes have the potential to erupt more magma than shorter radial dikes.

Evidence from Mount Adams volcano

Mount Adams, in the Cascade volcanic arc of southern Washington, USA, is well suited to test predictions of the proposed radial dike emplacement model. Eight andesitic eruptions have occurred at the stratovolcano in the past 15,000 years. Seven of the eruptions are inferred to have been fed by radial dikes, based on radially oriented cracks and eruptive fissures associated with the lava flow vents, and dike outcrops in the vent area of one andesite flow (Hildreth and Fierstein 1995, 1997).

A plot of lava flow volume versus distance between the vent and summit (determined from Hildreth and Fierstein 1995) for the seven dike-fed andesite lava flows supports our preferred model of radial dike emplacement (Fig. 7). Vents fed by inferred radial dikes tended to erupt greater volumes of lava with increasing distance from the summit of Mount Adams. In addition, Hildreth and Fierstein (1997) noted that the some of the flank vents are near the contact between the steep, rubbly, andesitic volcanic cone the more gently dipping apron of thicker lava flows. A neutral buoyancy zone or stress barrier at or near this contact may have caused the dikes to propagate laterally upon reaching the base of the cone. Finally, offset dike segments similar to those observed at Summer Coon occur at an intrusion that crops out in the vent of one flow at Mount Adams. At least 10 m of erosion have exposed "a pair of glassy dike-segment protrusions, which stand 4–8 m high" (Hildreth and Fierstein 1997). Little surface deformation has been documented above the inferred dikes (except some radial fissures and fractures on some of the Mount Adams andesite flows—see Hildreth and Fierstein 1997). However, numerical and analog models of dike intrusion (e.g. Pollard et al. 1983; Mastin and Pollard 1988) suggest that surface disruptions would have been measurable by deformation monitoring and visual observation prior to eruption.

Conclusions and suggestions for future work

Field observations of silicic dikes at Summer Coon lead us to propose a model for radial dike emplacement (Fig. 8) that predicts several features of magmatic intrusions at composite volcanoes:

1. Dike driving pressure increases with radial distance from the center of a host volcano, causing a corresponding increase in dike thickness. The thickening is probably caused by decreases in horizontal stress and elastic shear modulus under the outward-sloping flanks of the volcano.
2. The greatest volume of magma is generally available for eruption at the farthest extent of a radial dike (assuming only minor variations in temperature, viscosity and other factors between different dikes) because of heightened driving pressure with distance from the center of the volcano. As a result, the most voluminous eruptions from radial intrusions may occur around the flanks of a volcano, up to several kilometers from the summit, as is generally the case at Mt. Adams (Hildreth and Fierstein 1997). Radial dikes that feed surface vents on the upper

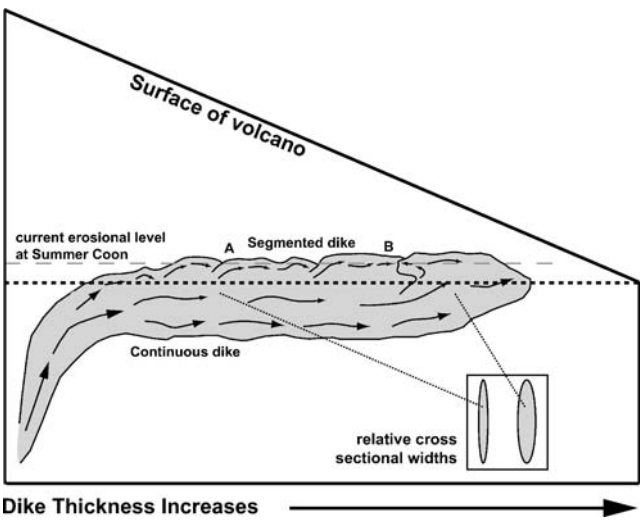

Fig. 8 Preferred model for radial dike emplacement based on observations at Summer Coon volcano. The present erosional surface at Summer Coon is indicated by the *gray dashed line*, and the stress discontinuity or neutral buoyancy zone (between the rocks of the basement and volcanic edifice), which marks the transition from upward to lateral dike propagation, is shown by the *black dotted line*. A radial dike is initiated at depth below the center of the volcano and propagates upwards along a steeply inclined path. Upon reaching the base of the volcanic cone the intrusion assumes a subhorizontal path and propagates radially away from the center of the volcano. The dike thickness increases with radial distance as the emplacement depth decreases due to the surface slope of the volcano (as indicated by *inset cross sections*) and the lower shear modulus of host rocks near the surface. The upper surface of the dike will be segmented as magma flows into coeval offset fractures. Segment tips proximal to the center of the volcano will not propagate towards one another (*location A*), whereas distal segment tips will propagate towards one another due to higher driving pressures (*location B*). The potential eruptive volume for an individual intrusion is greatest on the outer flanks of the volcano

flanks of the volcano will probably produce low-volume eruptions relative to low-flank dike-fed eruptions.

3. Silicic dikes will have a segmented geometry, possibly including multiple scales of offset segments. The cause of segmentation may result from a variety of mechanisms, including intrusion into dike-parallel joints that form ahead of the propagating dike.
4. Dike propagation is steep near the center of the volcano but becomes subhorizontal as the intrusion reaches the base of the edifice, probably due to a neutral buoyancy surface or a stress barrier near the base of the edifice (such effects could be caused by mechanical differences between the rocks of the basement and volcano, and/or stresses induced by the load of the volcano). Both factors would act to trap an intrusion at shallow depths. If the driving pressure in a trapped dike is sufficiently high, the intrusion would propagate laterally towards the flanks of the edifice.
5. The active intrusion of a silicic radial dike should be detectable by geophysical measurements, especially when an intrusion propagates subhorizontally away from the summit towards the flank of a volcano. Silicic dikes of similar thickness to those at Summer Coon should cause significant surface disruptions. The propagation and geometry of surface cracks away from the summit may indicate the location, form, and propagation rate of the dike, which may be used to forecast the timing and geometry of potential eruptive vents.

The characteristics of post-glacial andesitic flank eruptions at Mount Adams are consistent with the model for radial dike intrusion developed from Summer Coon. Our model, however, is based primarily on a detailed study of one eroded stratovolcano, and should be tested at other locations. Eroded volcanoes with exposed radial dike swarms that may be targeted for additional work include West Elk Peak in central Colorado (Gaskill et al. 1981), Mount Taylor in central New Mexico (Lipman et al. 1979), Sunlight volcano in western Wyoming (Parsons 1939), and San Francisco Mountain in northern Arizona (Holm 1988). If it proves accurate for other volcanic centers, the model presented in this paper could be used in support of hazards assessments of active composite volcanoes.

Acknowledgements This work was completed as part of Poland's doctoral dissertation, which was supported by a National Defense Science and Engineering Graduate Fellowship, and part of Moats' thesis, which was funded by Department of Energy grant DE-FG02-85ER13320 and NSF grant EAR8618365. Field work was funded by graduate research grants from the Geological Society of America, Scion Natural Science Association, and Colorado Scientific Society. David Pollard, Elissa Koenig, and Larry Mastin engaged in helpful discussions that substantially improved the quality of the manuscript. Aaron Lyman and Chantelle Lucas assisted with fieldwork. Willie Scott, Peter Lipman, Larry Mastin, David Pollard, Sven Morgan, Greg Valentine, and an anonymous reader provided constructive feedback.

References

Acocella V, Porrecam M, Neri M, Massimi E, Mattei M (2006) Propagation of dikes at Vesuvio (Italy) and the effect of Mt. Somma. Geophys Res Lett 33 DOI 10.1029/2005GL025590

Baer G (1991) Mechanisms of dike propagation in layered rocks and in massive, porous sedimentary rocks. J Geophys Res 96: 911–929

Baer G, Beyth M (1990) A mechanism of dyke segmentation in fractured host rock. In: Parker AJ, Rckwood PC, Tucker GH (eds) Mafic Dykes and emplacement mechanisms. AA Balkema Publishers, Rotterdam, pp. 3–11

Buck WR, Einarsson P, Brandsdottír B (2006) Tectonic stress and magma chamber size as controls on dike propagation: constraints from the 1975–1984 Krafla rifting episode. J Geophys Res 111: DOI 10.1029/2005JB003879

Chadwick WW Jr, Howard KA (1991) The pattern of circumferential and radial eruptive fissures on the volcanoes of Fernandina and Isabela islands, Galapagos. Bull Volcanol 53:259–275

Coombs ML, Gardner JE (2001) Shallow-storage conditions for the rhyolite of the 1912 eruption at Novarupta, Alaska. Geology 29:775–778

Corsaro RA, Cristofolini R, and Patanè L (1996) The 1669 eruption at Mount Etna—chronology, petrology, and geochemistry, with inferences on the magma sources and ascent mechanisms. Bull Volcanol 58:348–358

Delaney PT, Gartner AE (1997) Physical processes of shallow mafic dike emplacement near the San Rafael Swell, Utah. Geol Soc Am Bull 109:1177–1192

Delaney PT, Pollard DD (1981) Deformation of host rocks and flow of magma during growth of minette dikes and breccia bearing intrusions near Ship Rock, New Mexico. U.S. Geological Survey Professional Paper 1202

Delaney PT, Pollard DD, Ziony JI, McKee EH (1986) Field relations between dikes and joints; emplacement processes and paleostress analysis. J Geophys Res 91:4920–4938

Fink JH, Pollard DD (1983) Structural evidence for dikes beneath silicic domes, Medicine Lake Highland Volcano, California. Geology 11:458–461

Fiske RS, Jackson ED (1972) Orientation and growth of Hawaiian volcanic rifts: the effect of regional structure and gravitational stresses. Proc R Soc Lond A 329:299–326

Fukushima Y, Cayol V, Durand P (2005) Finding realistic dike models from interferometric synthetic aperture radar data: the February 2000 eruption of Piton de la Fournaise. J Geophys Res 110 DOI 10.1029/2004JB003268

Gaskill DL, Mutschler FE, Bartleson BL (1981) West Elk volcanic field, Gunnison and Delta counties, Colorado. In: Epis RC, Callender JF (eds) New Mexico Geological Society Guidebook, 32nd Field Conference, Western Slope Colorado. New Mexico Geological Society, Socorro

Gries RR (1985) San Juan Sag: cretaceous rocks in a volcanic-covered basin, south-central Colorado. Mt Geol 22:167–179

Gudmundsson A (1983) Form and dimensions of dykes in eastern Iceland. Tectonophysics 95:295–307

Gudmundsson A (1984) Formation of dykes, feeder-dykes, and the intrusion of dykes from magma chambers. Bull Volcanol 47:537–550

Gudmundsson A (1987) Lateral magma flow, caldera collapse, and a mechanism of large eruptions in Iceland. J Volcanol Geotherm Res 34:65–78

Gudmundsson A, Brenner SL (2004) How mechanical layering affects local stresses, unrests, and eruptions of volcanoes. Geophys Res Lett 31 DOI 10.1029/2004GL020083

Gudmundsson A, Brenner SL (2005) On the conditions of sheet injections and eruptions in stratovolcanoes. Bull Volcanol 67:768–782

Gudmundsson A, Marinoni LB, Marti J (1999) Injection and arrest of dykes: implications for volcanic hazards. J Volcanol Geotherm Res 88:1–13

Hashimoto M, Tada T (1992) A model for crustal deformations associated with the 1914 great eruption of Sakurajima volcano, Kagoshima, Japan. Tectonophys 205:427–436

Hildreth W, Fierstein J (1995) Geologic map of the Mount Adams volcanic field, cascade range of southern Washington. U.S. Geological Survey Miscellaneous Investigation I–2460

Hildreth W, Fierstein J (1997) Recent eruptions of Mount Adams, Washington Cascades, USA. Bull Volcanol 58:472–490

Hildreth W, Fierstein J (2000) The Katmai volcanic cluster and the great eruption of 1912. Geol Soc Am Bull 112:1594–1620

Holm RF (1988) Geologic map of San Francisco Mountain, Elden Mountain, and Dry Lake Hills, Coconino County, Arizona. U.S. Geological Survey Miscellaneous Investigation I–1663

Klügel A, Walter TR, Schwarz S, Geldmacher J (2005) Gravitational spreading causes en-echelon diking along a rift zone of Madeira Archipelago: an experimental approach and implications for magma transport. Bull Volcanol 68:37–46

Lacey A, Ockendon JR, Turcotte DL (1981) On the geometrical form of volcanoes. Earth Planet Sci Lett 54:139–143

Lipman PW (1968) Geology of the Summer Coon volcanic center, eastern San Juan Mountains, Colorado. Colo Sch Mines Q 63: 211–236

Lipman PW (1976) Geological map of the Del Norte area, eastern San Juan mountains, Colorado. U.S. Geological Survey Miscellaneous Investigation I-952

Lipman PW, Steven TA, Mehnert LH (1970) Volcanic history of the San Juan mountains, Colorado, as indicated by potassium–argon dating. Geol Soc Am Bull 81:2329–2352

Lipman PW, Pallister JS, Sargent KA (1979) Geologic Map of the Mount Taylor Quadrangle, Valencia County, New Mexico. U.S. Geological Survey Geologic Quadrangle Map GQ–1523

Martel SJ (2000) Modeling elastic stresses in long ridges with the displacement discontinuity method. Pure Appl Geophys 157: 1039–1057

Mastin LG, Pollard DD (1988) Surface deformation and shallow dike intrusion processes at Inyo Craters, Long Valley, California. J Geophys Res 93:221–235

Mertzman SA (1971) The Summer Coon volcano, eastern San Juan mountains, Colorado. In: James HL (ed) New Mexico Geological Society Guidebook, 22nd Field Conference, San Luis Basin. New Mexico Geological Society, Socorro, pp. 265–272

Moats WP (1990) Geometry and emplacement of silicic dikes at Summer Coon Volcano, Rio Grande and Saguache counties, Colorado. MS thesis, Arizona State University, Tempe

Morita Y, Nakao S, Hayashi Y (2006) A quantitative approach to the dike intrusion process inferred from a joint analysis of geodetic and seismological data for the 1998 earthquake swarm off the east coast of Izu Peninsula, central Japan. J Geophys Res 111 DOI 10.1029/2005JB003860

Muller OH, Pollard DD (1977) The stress state near Spanish Peaks, Colorado, determined from a dike pattern. Pure Appl Geophys 115:69–86

Nakamura K (1977) Volcanoes as possible indicators of tectonic stress orientation; principle and proposal. J Volcanol Geotherm Res 2:1–16

Newhall CG, Dzurisin D (1988) Historical unrest at large calderas of the world. US Geol Surv Bull 1855

Nunn JA (1996) Buoyancy-driven propagation of isolated fluid-filled fractures: implications for fluid transport in the Gulf of Mexico. J Geophys Res 101:2963–2970

Obert L, Duvall WI (1967) Rock mechanics and the design of structures in rock. Wiley, New York

Ode H (1957) Mechanical analysis of the dike pattern of the Spanish Peaks area, Colorado. Geol Soc Am Bull 68:567–576

Olson JE, Pollard DD (1989) Inferring paleostress from natural fracture patterns: a new method. Geology 17:345–348

Olson JE, Pollard DD (1991) The initiation and growth of en echelon veins. J Struct Geol 13:595–608

Omori, F (1915) The eruption of Sakura-jima, 1914. Bull Seismol Soc Am 5:71–95

Parsons WH (1939) Volcanic centers of the Sunlight area Park County, Wyoming. J Geology 47:1–26

Peltier A, Ferrnzzini V, Staudacher T, Bachèlery P (2005) Imaging the dynamics of dyke propagation prior to the 2000–2003 flank eruptions at Piton de la Fourniase, Reunion Island. Geophys Res Lett 32 DOI 10.1029/2005GL023720

Perry FV, Woldegabriel G, Valentine GA, Desmarais EK, Heiken G, Heizler M, Yamakawa M, Umeda K (1999) High-level radioactive waste disposal and volcanic hazard in Japan—a natural analog study of Summer Coon volcano, Colorado. Geol Soc Am Abstracts with Programs 31:A478

Perry FV, Valentine GA, Desmarais EK, WoldeGabriel G (2001) Probabilistic assessment of volcanic hazard to radioactive waste repositories in Japan: intersection by a dike from a nearby composite volcano. Geology 29:255–258

Pinel V, Jaupart C (2000) The effect of edifice load on magma ascent beneath a volcano. Phil Trans R Soc Lond A 358:1515–1532

Pinel V, Jaupart C (2004) Magma storage and horizontal dike injection beneath a volcanic edifice. Earth Planet Sci Lett 221: 245–262

Poland MP, Fink JH, Tauxe L (2004) Patterns of magma flow in segmented silicic dikes at Summer Coon volcano, Colorado: AMS and thin section analysis. Earth Planet Sci Lett 219:155–169

Pollard DD (1987) Elementary fracture mechanics applied to the structural interpretation of dykes. In: Halls HC, Fahrig WF (eds) Mafic Dike Swarms, Geological Association of Canada Special Paper 34, pp. 5–24

Pollard DD, Holzhausen G (1979) On the mechanical interaction between a fluid-filled crack and the Earth's surface. Tectonophysics 53:27–57

Pollard DD, Muller OH (1976) The effect of gradients in regional stress and magma pressure on the form of sheet intrusions in cross section. J Geophys Res 81:975–984

Pollard DD, Muller OH, Dockstader DR (1975) The form and growth of fingered sheet intrusions. Geol Soc Am Bull 86:351–363

Pollard DD, Segall P, Delaney PT (1982) Formation and interpretation of dilatant echelon cracks. Geol Soc Am Bull 93:1291–1303

Pollard DD, Delaney PT, Duffield WA, Endo ET, Okamura AT (1983) Surface deformation in volcanic rift zones. Tectonophysics 94: 541–584

Reches Z, Fink J (1988) The mechanism of intrusion of the Inyo Dike, Long Valley Caldera, California. J Geophys Res 93:4321–4334

Richter DH, Eaton JP, Murata KJ, Ault WU, Kirvoy HL (1970) Chronological narrative of the 1959–1960 eruption of Kilauea Volcano, Hawaii. U.S. Geological Survey Professional Paper 537-E

Rivalta E, Dahm T (2006) Acceleration of buoyancy-driven fractures and magmatic dikes beneath the free surface. Geophys J Int 166:1424–1439

Rivalta E, Böttinger M, Dahm T (2005) Buoyancy-driven fracture ascent: Experiments in layered gelatine. J Volcanol Geotherm Res 144:273–285

Rubin AM (1990) A comparison of rift-zone tectonics in Iceland and Hawaii. Bull Volcanol 52:302–319

Rubin AM (1993) On the thermal viability of dikes leaving magma chambers. Geophys Res Lett 20:257–260

Rubin AM (1995) Getting granite dikes out of the source region. J Geophys Res 100:5911–5929

Rubin AM, Pollard DD (1987) Origins of blade-like dikes in volcanic rift zones. In: Decker RW, Wright TL, Stauffer, PH (eds) Volcanism in Hawaii. U.S. Geological Survey Professional Paper 1350, pp. 1449–1470

Rubin AM, Pollard DD (1988) Dike-induced faulting in rift zones of Iceland and Afar. Geology 16:413–417

Ryan MP (1987) Neutral buoyancy and the mechanical evolution of magmatic systems, in Mysen BO (ed) Magmatic Processes—Physiochemical Principles, The Geochemical Society, Special Publication No. 1, pp. 259–287

Saunders SJ (2001) The shallow plumbing system of Rabaul caldera—a partially intruded ring fault? Bull Volcanol 63:406–420

Schultz RA (1993) Brittle strength of basaltic rock masses with applications to Venus. J Geophys Res 98:883–895

Sherrod DR, Smith JG (1990) Quaternary extrusion rates of the Cascade Range, northwestern United States and southern British Columbia. J Geophys Res 95:465–474

Smith RP (1987) Dyke emplacement at Spanish Peaks, Colorado. In: Halls HC, Fahrig WF (eds) Mafic Dyke Swarms. Geological Association of Canada Special Paper 34, pp. 47–54

Smith RL, Bailey RA (1968) Resurgent cauldrons. In: Coats RR, Hay RL, Anderson CA (eds) Studies in Volcanology—a memoir in honor of Howel Williams, Geological Society of America Memoir 116, pp. 613–662

Sommer E (1969) Formation of fracture 'lances' in glass. Engineering Fracture Mechanics 1:539–546

Sturkell E, Einarsson P, Sigmundsson F, Geirsson H, Ólafsson H, Pedersen R, de Zeeuw-van Dalfsen E, Linde AT, Sacks IS, Stefánsson R (2006) Volcano geodesy and magma dynamics in Iceland. J Volcanol Geotherm Res 150:14–34

Valentine GA, Krough KEC (2006) Emplacement of shallow dikes and sills beneath a small basaltic volcanic center—the role of pre-existing structure (Paiute Ridge, Southern Nevada, USA). Earth Planet Sci Lett 246:217–230

Valentine GA, Perry FV, WoldeGabriel G (2000) Field characteristics of deposits form spatter-rich pyroclastic ensity currents at Summer Coon volcano, Colorado. J Volcanol Geotherm Res 104:187–199

Walker GPL (1987) The dike complex of Koolau volcano, Oahu: internal structure of a Hawaiian rift zone. In: Decker RW, Wright TL, Stauffer PH (eds) Volcanism in Hawaii. U.S. Geological Survey Professional Paper 1350, pp. 961–993

Weertman J (1971) Theory of water-filled crevasses in glaciers applied to vertical magma transport beneath oceanic ridges. J Geophys Res 76:1171–1183

Wood CA, Kienle J (1990) Volcanoes of North America. Cambridge University Press, New York

Yamashina K, Shimizu H (1999) Crustal deformation in the mid-May 1991 crisis preceding the extrusion of a dacite lava dome at Unzen volcano, Japan. J Volcanol Geotherm Res 89:43–55

Yokoyama I (1986) Crustal deformation caused by the 1914 eruption of Sakurajima volcano, Japan and its secular changes. J Volcanol Geotherm Res 30:283–302